

Fe-Mediated ICAR ATRP of Styrene and Acrylonitrile in Polyethylene Glycol

Guo-Xiang Wang,¹ Mang Lu,² Zhao-Hui Hou,¹ Yong Gao,³ Li-Chao Liu,¹ Hu Wu¹

¹College of Chemistry and Chemical Engineering, Hunan Institute of Science and Technology, Yueyang 414006, Hunan, People's Republic of China

²School of Materials Science and Engineering, Jingdezhen Ceramic Institute, Jingdezhen 333403, Jiangxi, People's Republic of China

³College of Chemistry, Xiangtan University, Xiangtan 411105, Hunan, People's Republic of China

Correspondence to: G.-X. Wang (E-mail: wanggxwz1@163.com) or Z.-H. Hou (E-mail: zhqh96@163.com)

ABSTRACT: In this contribution, random copolymers of p(styrene-co-acrylonitrile) via initiators for continuous activator regeneration (ICAR) in atom transfer radical polymerization (ATRP) (ICAR ATRP) of styrene and acrylonitrile (SAN) were synthesized at 90°C in low molecular weight polyethylene glycol (PEG-400) using CCl₄ as initiator, FeCl₃·6H₂O as catalyst, succinic acid as ligand and thermal radical initiator azobisisobutyronitrile (AIBN) as thermal free radical initiator. In this system, well-defined copolymer of SAN was achieved. The kinetics results showed that the copolymerization rate obeyed first-order kinetics model with respect to the monomer concentration, and a linear increase of the molecular weights with the increasing of monomer conversion with narrow molecular weight distribution was observed in the range of 1.1–1.5. The conversion decreased with increasing the amount of FeCl₃·6H₂O and increased with increasing the molar ratio of [St]₀/[AN]₀/[CCl₄]₀ and temperature. AIBN has a profound effect on the polymerization. The activation energy was 55.67 kJ mol⁻¹. The living character of copolymerization was confirmed by chain extension experiment. The resultant random copolymer was characterized by ¹H-NMR and GPC. © 2013 Wiley Periodicals, Inc. *J. Appl. Polym. Sci.* **2014**, *131*, 40135.

KEYWORDS: copolymer; kinetic; living radical polymerization; catalysts

Received 29 June 2013; accepted 26 October 2013

DOI: 10.1002/app.40135

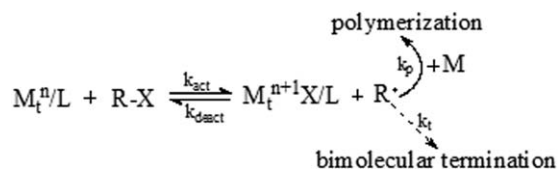
INTRODUCTION

Atom transfer radical polymerization (ATRP) is a potential technique of choice for the preparation of polymers with unique and well-defined architectures due to its relatively mild reaction conditions since its founding in 1995.^{1–4} ATRP was mediated transition metal catalyst and set up a dynamic equilibrium between active species and dormant species. The main disadvantage with conventional ATRP is that equimolar amounts of initiator (alkyl halide) and mediator must be used.¹ The mechanism of ATRP is illustrated in Scheme 1.

To overcome these limits, some improved ATRP techniques have been developed, such as Activators generated by electron transfer for atom transfer radical polymerization (AGET ATRP), ICAR ATRP. Compared to the conventional ATRP, oxidatively stable transition metal catalysts are used in AGET ATRP system. The higher oxidation state transition metal is reduced by reducing agent to form active catalyst species that are unable to initiate new chains. This process is finished through electron

transfer other than by organic radicals. The advantages of AGET ATRP are that the catalyst is easily prepared, stored, and handled. The mechanism of AGET ATRP is illustrated in Scheme 2.

Recently, an improved ATRP technique, ICAR ATRP has been developed.^{5–8} This technique has potential application in industry because the polymerization was conducted with a very active transition metal catalyst in a tiny amount in the presence of the conventional radical initiator azobisisobutyronitrile (AIBN). In a typical ICAR ATRP, radicals are continuously generated by the decomposition of conventional free radical initiator and the reduction of higher oxidation transition metal salts to lower oxidation transition metal salts. Then the process is the same as that in a normal ATRP procedure. The polymerization rate depends heavily on the decomposition kinetics of the additional initiator, as decomposition can dominate the active radical concentration. There is an apparent limitation in ICAR ATRP system, namely block copolymers cannot be prepared because the radicals generated thermally (Sty) or from a radical source may

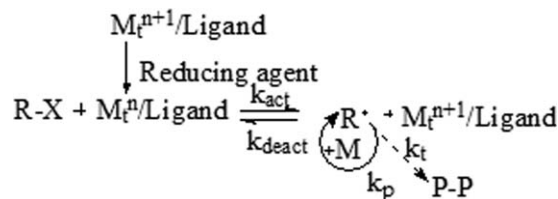


Scheme 1. The mechanism for ATRP.

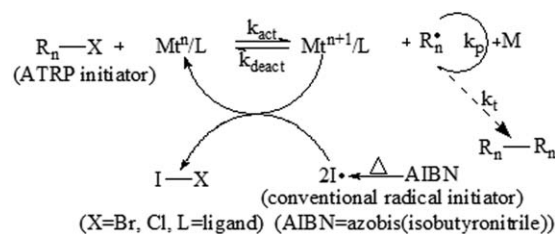
initiate new polymer chains. Thus, reducing agents should be used that cannot initiate polymerization.⁹ The mechanism of ICAR ATRP is illustrated in Scheme 3.

Catalysts and ligands play a vital role in determining the overall activity of the catalyst in ICAR ATRP. Among the transition metals catalysts in ATRP, iron catalyst complexes are the most abundant and environmentally friendly transition metals. Some excellent Fe-mediated ICAR ATRPs have been reported.^{10–12} The main role of the ligand in ATRP is to solubilize the transition-metal salt in the organic media and to adjust the redox potential of the metal center for appropriate reactivity and dynamics for the atom transfer. It adjusts the redox potential around the metal center which affects the reactivity and equilibrium dynamics of the atom transfer process. Furthermore, the ligands can facilitate the removal and recycling of the catalyst allowing the immobilization of the catalyst. Various ligands have been used in Fe-mediated ICAR ATRP system, especially based on nitrogen and phosphorous, for example, triphenylphosphine (PPh₃),¹⁰ tris(3,6-dioxahexyl) amine (TDA-1),¹¹ ethyl 2-bromo-2-phenylacetate (EBrPA),¹² and tetrabutylammonium bromide (TBABr).^{12–14} However, these ligands have some disadvantages, such as expensiveness or environmental harm to health. Succinic acid (SA) has been used as an environmentally friendly ligand in ICAR ATRP by our groups.^{15–17}

It is very desirable to perform well-controlled ATRP in the most environmentally friendly and inexpensive solvents. For example, ionic liquid, super CO₂. However, they have some disadvantages: preparation of difficulty, high price and the limited knowledge on the toxicity about ionic liquid. Compared to ionic liquid and super CO₂, PEGs have been approved by the Food and Administration's (FDA's) for internal consumption. Furthermore, PEGs are more environmentally friendly and inexpensively solvents and have been applied in organic synthesis,¹⁸ separating analytes,¹⁹ phase-transfer catalyst,²⁰ and aqueous biphasic reactive extraction (ABRE).²¹ Recently, low molecular weight PEGs have attracted increasing interest as novel solvents due to their good biocompatibility, low cost, low toxicity to human beings and environment, nonvolatile, and potential application in the field of polymer chemistry.^{22,23} In addition, PEGs have generally been touted as potential replacements for



Scheme 2. The mechanism for AGET ATRP.



Scheme 3. The mechanism for ICAR ATRP.

volatile organic solvents in many applications. PEGs as solvents in living radical polymerization were first reported by Perrier et al.²³ in 2004 in the CuCl/N-(*n*-pentyl)-2-pyridylmethanimine catalyzed polymerization of MMA and St using ethyl 2-bromoisobutyrate (EBiB) as an initiator with the molar ratio of $[M]/[I]/[Cu(I)]/[Cu(II)]/[L] = 100 : 1 : 0.97 : 0.03 : 2$ and $[M]:[I]:[Cu(I)]:[L] = 100 : 1 : 1 : 2$, respectively. Higher rate of polymerization of methyl methacrylate was found than that in toluene, but the rate was slower for styrene in PEG-400 than that in xylene. In another example, Cu-mediated AGET ATRP of MMA has been successfully performed in PEG-600 using CuCl₂ or CuBr₂ as the catalyst, ethyl 2-bromoisobutyrate (EBiB) as initiator and *N,N,N',N'*-tetramethylethylenediamine (TMEDA) as both ligand and reducing agent,²² the polymerization was well-controlled with low M_w/M_n (PDI < 1.2).

Copolymer of styrene and acrylonitrile (SAN) has been widely applied in many fields due to its superior mechanical properties, chemical resistance, heat resistance and optical properties, and easy processability. The copolymerization of SAN in bulk,²⁴ solution,²⁵ suspension,²⁶ emulsion,²⁷ or microemulsion²⁸ systems has been extensively investigated with conventional radical polymerization methods. However, little work about controlled and living copolymerization of SAN has been reported.^{29–36}

To the best of the authors' knowledge, there is no report on Fe-mediated ICAR ATRP in low molecular weight PEG. In this work, PEG was used as solvent in Fe-mediated ICAR ATRP of styrene (St) and acrylonitrile (AN). Fe-mediated ICAR ATRP of St and AN was firstly performed in PEG-400 using FeCl₃·6H₂O/SA as a catalyst, AIBN as a thermal free radical initiator, and CCl₄ as an ATRP initiator.

EXPERIMENTAL

Materials

Styrene (Analytic Reagent grade, AR grade) was purchased from Tianjin Fuchen Chemical Reagents Factory, China. It was distilled under reduced pressure prior to use. Acrylonitrile (Analytic Reagent grade, AR grade) was purchased from Tianjin Bodi Chemical Holding, China. It was distilled under reduced pressure prior to use. AIBN, obtained from Shanghai Chemical Holding, China, was recrystallized twice from methanol. Ferric chloride hexahydrate was purchased from Shanghai Qingfeng Chemical Factory, China. Succinic acid, (SA, AR grade) was obtained from Chongqin Chuandong Chemical (group), and were used as received. Carbon tetrachloride (CCl₄, 99%), obtained from Hunan HuiHong Reagent, was used without further purification. PEG-400 was obtained from Sinopharm

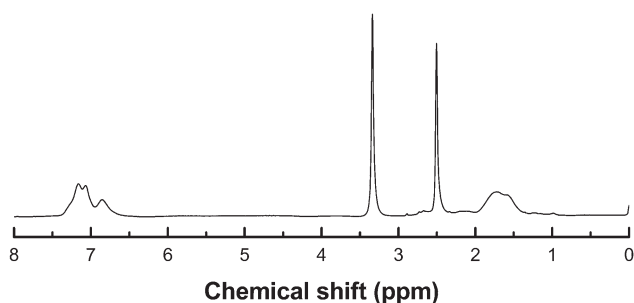


Figure 1. ^1H -NMR spectrum of SAN. Polymerization conditions: $[\text{St}]_0/[\text{AN}]_0/[\text{CCl}_4]_0/[\text{FeCl}_3 \cdot 6\text{H}_2\text{O}]_0/[\text{SA}]_0/[\text{AIBN}]_0 = 225 : 135 : 1 : 0.4 : 0.8 : 0.1$ in 20 mL PEG-400 at 60°C . Polymerization time = 6 h, Conversion = 17%.

Chemical Reagent, Shanghai, China, were used as received. Other reagents were used as received.

Polymerization

The ICAR ATRP of St and AN was performed with the ratio of $[\text{St}]_0/[\text{AN}]_0/[\text{CCl}_4]_0/[\text{FeCl}_3 \cdot 6\text{H}_2\text{O}]_0/[\text{SA}]_0/[\text{AIBN}]_0 = 225 : 135 : 1 : 0.4 : 0.8 : 0.1$ under nitrogen in a 100-mL three-neck round-bottomed flask equipped with a magnetic stirring bar. A typical example of the general procedure is as follows: St (0.0225 mol, 2.3400 g), AN (0.0135 mol, 0.7163 g), CCl_4 (1×10^{-4} mol, 0.0154 g), $\text{FeCl}_3 \cdot 6\text{H}_2\text{O}$ (4×10^{-5} mol, 0.1081 g), SA (8×10^{-5} mol, 0.094 g), AIBN (1×10^{-5} mol, 0.0164 g), and 20 mL PEG-400 were added to the flask under stirring until the homogeneous solution was formed. The flask was sealed after degassed with nitrogen and then placed in an oil bath held by a thermostat at the desired reaction temperature to polymerize under stirring. After the desired polymerization time, the flask was cooled by immersing into ice water. The reactant was pored into a large amount of methanol for precipitation. The obtained SAN was vacuum-dried at 60°C for 1 day. Monomer conversion was determined by gravimetry.

Chain Extension

PSt was synthesized by Fe-mediated ICAR ATRP of St and then the obtained PSt was used macroinitiator for the ICAR ATRP of St and AN in PEG-400 at 90°C . The procedure is as follows: a predetermined quantity of PSt was added to a dried 100-mL three-neck round-bottomed flask, and then the predetermined quantity of St, AN, $\text{FeCl}_3 \cdot 6\text{H}_2\text{O}$, SA, AIBN, and 20 mL PEG-400 was added. The rest of the procedure was the same as that

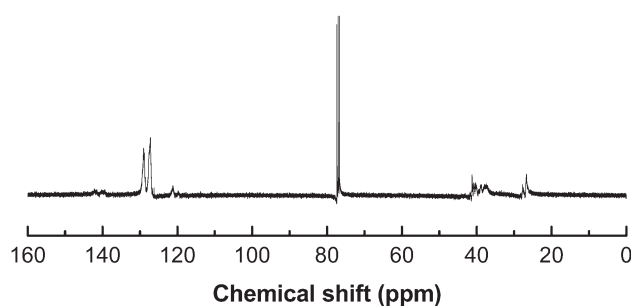


Figure 2. ^{13}C -NMR spectrum of SAN. The polymerization conditions were the same as Figure 1.

described above. The chain-extension polymerization was performed under stirring at 90°C .

Measurements

A Waters 1515 gel permeation chromatography (GPC) was used to evaluate the number-average molecular weight ($M_{n,\text{GPC}}$) and molecular weight distribution (M_w/M_n) of the resultant copolymer. GPC was equipped with a refractive index detector, using HR1, HR3, and HR4 columns. Polystyrene standard samples with molecular weight range of 100–500,000 were used to calibrate the columns. A mobile phase, tetrahydrofuran, was used at a flow rate of 1.0 mL min^{-1} . The column temperature was kept at 30°C .

^1H -NMR and ^{13}C -NMR spectra were recorded on a Bruker 400 MHz Spectrometer instrument. CDCl_3 was used as the deuterated reagents and tetramethylsilane (TMS) was used as the internal standard at ambient temperature.

RESULTS AND DISCUSSION

^1H -NMR and ^{13}C -NMR spectra

The ^1H -NMR and ^{13}C -NMR spectra of SAN prepared in PEG-400 by Fe-mediated ICAR ATRP of SAN with AIBN as a thermal free radical initiator at 90°C are shown in Figures 1 and 2. In Figure 1, the chemical shift at 6.57–7.66 ppm belonged to the protons of the phenyl. The weak chemical signals situated at 4.5–5.3 ppm were proton of end group of $-\text{CHCl}$. However, the methylene and methine protons of the copolymer were overlapped in the region 1.2–3.1 ppm. In Figure 2, the chemical shift at 26.5–28.9 ppm corresponded to the methine protons of the copolymer. The signals at 36.9–43.7 ppm were attributed to the protons of the methylene protons of the copolymer. The chemical shifts at 119.1–122.3 ppm were assigned to nitrile carbon protons of the copolymer. The signals at 126.3–130.7 ppm were contributed to the aromatic ring carbons protons of the copolymer. As analyzed above, the obtained polymer was SAN copolymer.

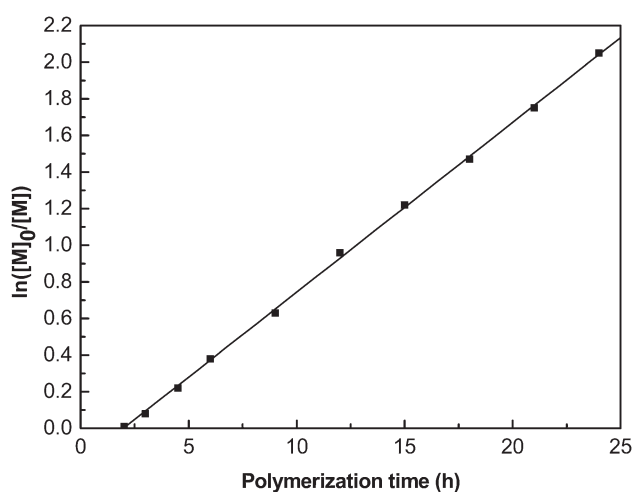


Figure 3. Semilogarithmic kinetic plot for Fe-mediated ICAR ATRP of SAN. Polymerization conditions: $[\text{St}]_0/[\text{AN}]_0/[\text{CCl}_4]_0/[\text{FeCl}_3 \cdot 6\text{H}_2\text{O}]_0/[\text{PEG-1000}]_0/[\text{AIBN}]_0 = 225 : 135 : 1 : 0.4 : 0.8 : 0.1$ in 20 mL PEG-400 at 90°C .

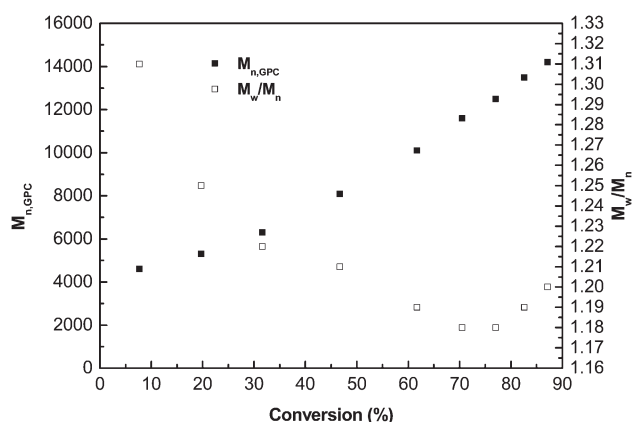


Figure 4. Dependence of molecular weight and M_w/M_n on monomer conversion. The experimental conditions were the same as Figure 3.

ICAR ATRP of SAN

The ICAR ATRP of St and AN was first investigated in 20 mL PEG-400 with the molar ratio of $[St]_0/[AN]_0/[CCl_4]_0/[FeCl_3 \cdot 6H_2O]_0/[SA]_0/[AIBN]_0 = 225 : 135 : 1 : 0.4 : 0.8 : 0.1$ at $90^\circ C$. It can be seen from Figure 3 that, the curve of $\ln([M]_0/[M])$ versus time keeps linear relationship up to 76% or so. The kinetic plots indicated first-order kinetics and that the concentration of propagating radicals remained constant during the polymerization process. An induction period of about 1.9 h was observed at the beginning of polymerization. The induction period was due to the decomposition of AIBN and to the establishment of the dynamic equilibrium between Fe(III) species and Fe(II) species. However, the equilibrium was established as the polymerization reaction proceeded. The apparent rate constant (k_{app}) ($k_{app} = d\ln([M]_0/[M])$) was $2.57 \times 10^{-5} s^{-1}$.

Figure 4 shows the relationship of dependence of number-average molecular weights as a function of monomer conversion for ICAR ATRP of SAN in PEG-400 at $90^\circ C$. As shown in Figure 4, the experimental molecular weight values of $M_{n,GPC}$ increased linearly with conversion and exhibited narrow molecular weight distribution. M_w/M_n values were lower than 1.33 in all cases. The results indicated that the polymerization was well-controlled. In comparison with reverse ATRP of St and AN

(35), the M_w/M_n values were slightly lower. Furthermore, the polymerization rate was slower than that of reverse ATRP of St and AN, which may be due to different reaction systems.

From the above discussion, it can be concluded that the Fe-mediated ICAR ATRP of St and AN in PEG-400 remained the controllable and living radical polymerization characteristics of ATRP.

The Effect of Amount of $FeCl_3 \cdot 6H_2O$ on the ICAR ATRP of SAN

The catalyst $FeCl_3 \cdot 6H_2O$ played an important role in ATRP. The polymerization proceeded in an uncontrolled manner when there was no catalyst or insufficient catalyst. However, the final polymer could be contaminated when excess catalyst was used. To investigate the effect of $FeCl_3 \cdot 6H_2O$ on the ICAR ATRP of SAN, a series of experiments were performed in PEG-400 with different amounts of $FeCl_3 \cdot 6H_2O$. The results are listed in Table I.

As can be seen from Table I, the polymerization proceeded in an uncontrolled manner in the absence of $FeCl_3 \cdot 6H_2O$ because of the broad molecular weight distribution ($M_w/M_n = 1.68$). When the molar ratio of $[CCl_4]_0/[FeCl_3 \cdot 6H_2O]$ was 1 : 0.01, a higher M_w/M_n value was obtained, indicating the polymerization remained uncontrolled. When the molar ratio of $[CCl_4]_0/[FeCl_3 \cdot 6H_2O]$ was 1 : 0.02, a lower M_w/M_n value was obtained, indicating that the polymerization proceeded in a controlled manner. Furthermore, the conversion rate decreased with the increase of the content of $[FeCl_3 \cdot 6H_2O]$, indicating the polymerization rate was controlled via increasing the content of catalyst. The apparent rate constants (k_{app}) values (in Table I), which were determined from the slope of the first-order kinetics plots, changed from $8.44 \times 10^{-5} s^{-1}$ to $1.02 \times 10^{-5} s^{-1}$ when the molar ratio of $[CCl_4]_0/[FeCl_3 \cdot 6H_2O]$ changed from 1 : 0 to 1 : 4. It was further verified that the content of catalyst played a vital role in the ICAR ATRP of St and AN.

The Effect of Different Ratios of $[St]_0/[AN]_0/[CCl_4]_0$ on the ICAR ATRP of SAN

To obtain a better understanding of this polymerization system, a series of the different ratios of $[St]_0/[AN]_0/[CCl_4]_0$ for Fe-mediated ICAR ATRP of SAN were applied. The results are shown in Table II. As can be seen, the polymerization rate increased when the molar ratio of $[St]_0/[AN]_0/[CCl_4]_0$ changed

Table I. Effect of Amount of $FeCl_3 \cdot 6H_2O$ on Fe-Mediated ICAR ATRP of SAN^a

Entry	$[CCl_4]_0/[FeCl_3 \cdot 6H_2O]_0$	Time (h)	Conversion (%)	$M_{n,GPC}$ ($g \text{ mol}^{-1}$)	M_w/M_n	k_{app} (s^{-1}) ^b
1	1 : 0	15	98.95	103,600	1.68	8.44×10^{-5}
2	1 : 0.01	15	91.23	36,500	1.55	4.51×10^{-5}
3	1 : 0.02	15	86.62	28,400	1.25	3.72×10^{-5}
4	1 : 0.1	15	78.36	22,430	1.21	2.83×10^{-5}
5	1 : 0.4	15	70.55	11,600	1.18	2.26×10^{-5}
6	1 : 1	15	58.32	10,700	1.17	1.62×10^{-5}
7	1 : 2	15	50.26	9500	1.17	1.29×10^{-5}
8	1.4	15	42.32	8300	1.17	1.02×10^{-5}

^a Polymerization conditions: $[St]_0/[AN]_0/[CCl_4]_0/[SA]_0/[AIBN]_0 = 225 : 135 : 1 : 0.8 : 0.1$. The polymerization temperature = $90^\circ C$, 20 mL PEG-400.

^b Determined from the slope of the first-order kinetics plot.

Table II. Effects of Molar Ratios of $[St]_0/[AN]_0/[CCl_4]_0$ on Fe-Mediated ICAR ATRP of SAN^a

Entry	$[St]_0/[AN]_0/[CCl_4]_0$	Time (h)	Conversion (%)	$M_{n,GPC}$ (g mol ⁻¹)	M_w/M_n	k_{app} (s ⁻¹) ^b
1	150 : 90 : 1	12	49.23	9100	1.23	1.57×10^{-5}
2	225 : 135 : 1	12	61.71	10,100	1.19	2.22×10^{-5}
3	750 : 450 : 1	12	67.84	11,200	1.21	2.63×10^{-5}
4	1500 : 900 : 1	12	73.44	14,800	1.22	3.07×10^{-5}
5	3000 : 1800 : 1	12	81.57	16,600	1.21	3.91×10^{-5}

^a Polymerization conditions: $[CCl_4]_0/[FeCl_3 \cdot 6H_2O]_0/[SA]_0/[AIBN]_0 = 1 : 0.4 : 0.8 : 0.1$. The polymerization temperature = 90°C, 20 mL PEG-400.

^b Determined from the slope of the first-order kinetics plot.

Table III. Effects of Different Amount of AIBN on ICAR ATRP of SAN^a

Entry	R	Time (h)	Conversion (%)	$M_{n,GPC}$ (g mol ⁻¹)	M_w/M_n	k_{app} (s ⁻¹) ^b
1	225 : 135 : 1 : 0.4 : 0.8 : 0	9	18.22	4400	1.32	6.21×10^{-6}
2	225 : 135 : 1 : 0.4 : 0.8 : 0.1	9	46.72	8100	1.21	1.94×10^{-5}
3	225 : 135 : 1 : 0.4 : 0.8 : 0.2	9	50.17	9600	1.24	2.15×10^{-5}
4	225 : 135 : 1 : 0.4 : 0.8 : 0.4	9	58.74	10,800	1.27	2.73×10^{-5}
5	225 : 135 : 1 : 0.4 : 0.8 : 0.5	9	66.53	11,700	1.42	3.38×10^{-5}

^a Polymerization conditions: $R = [St]_0/[AN]_0/[CCl_4]_0/[FeCl_3 \cdot 6H_2O]_0/[SA]_0/[AIBN]_0$. The polymerization temperature = 90°C, 20 mL PEG-400.

^b Determined from the slope of the first-order kinetics plot.

from 150 : 90 : 1 to 3000 : 1800 : 1. In addition, the apparent constant increased from $1.57 \times 10^{-5} \text{ s}^{-1}$ to $3.91 \times 10^{-5} \text{ s}^{-1}$ when the molar ratio of $[St]_0/[AN]_0/[CCl_4]_0$ changed from 150 : 90 : 1 to 3000 : 1800 : 1, indicating that increasing the monomer concentration would increase the polymerization rate. However, the M_w/M_n values kept narrow ($1.19 < M_w/M_n < 1.23$). All these results indicated that this polymerization system has high activity, even under higher feed ratios of $[St]_0/[AN]_0/[CCl_4]_0 = 3000 : 1800 : 1$.

The Effect of Amount of AIBN on the ICAR ATRP of SAN

For typical ICAR ATRP, the activators are continuously generated by *in situ* reduction high oxidation transition metal with the thermal initiator AIBN. To further investigate the effect of amount of AIBN on the ICAR ATRP of SAN, different amounts of AIBN were added to the reaction system. As can be seen from Table III, the polymerization conversion increased from 18.22 to 66.53% when the molar ratio of R changed from 225 : 135 : 1 : 0.4 : 1 : 0 to 225 : 135 : 1 : 0.4 : 1.4 : 0.5. This was a result of more radicals being generated by the decomposition of AIBN. According to the mechanism of ICAR ATRP, increasing

the content of AIBN resulted in the higher concentration of Fe(II)/SA produced by the reduction of Fe(III)/SA complex, and then increased concentrations of the propagating radicals in the polymerization system, resulting in the increase of polymerization rate. It further confirmed that the values of the apparent rate constants changed from $6.21 \times 10^{-6} \text{ s}^{-1}$ to $2.73 \times 10^{-5} \text{ s}^{-1}$. However, the M_w/M_n values remained narrow ($1.32 < M_w/M_n < 1.27$) when R changed from 225 : 135 : 1 : 0.4 : 0.8 : 0 to 225 : 135 : 1 : 0.4 : 0.8 : 0.4. The M_w/M_n values became broad ($M_w/M_n = 1.42$) when R was 225 : 135 : 1 : 0.4 : 0.8 : 0.5, indicating that excess AIBN resulted in some side reactions, especially at the beginning of polymerization.

The Effect of Polymerization Temperature on the ICAR ATRP of SAN

From the mechanism of ICAR ATRP shown in Scheme 3, the decomposition rate of thermal initiator AIBN was affected by temperature. The higher the temperature is, the faster the rate of initiator decomposition and the larger the number of free radicals available in solution, so reaction temperature controls the concentrations of propagating radicals. The effects of

Table IV. Effects of Polymerization Temperature on ICAR ATRP of SAN^a

Entry	Temperature (°C)	Time (h)	Conversion (%)	$M_{n,GPC}$ (g mol ⁻¹)	M_w/M_n	k_{app} (s ⁻¹) ^b
1	70	26	48.62	7900	1.31	7.11×10^{-6}
2	80	17	53.15	7600	1.27	1.24×10^{-5}
3	90	10	52.33	8800	1.20	2.06×10^{-5}
4	100	6	51.17	8300	1.34	3.32×10^{-5}

^a Polymerization conditions: $[St]_0/[AN]_0/[CCl_4]_0/[FeCl_3 \cdot 6H_2O]_0/[SA]_0/[AIBN]_0 = 225 : 135 : 1 : 0.4 : 0.8 : 0.1$, 20 mL PEG-400.

^b Determined from the slope of the first-order kinetics plot.

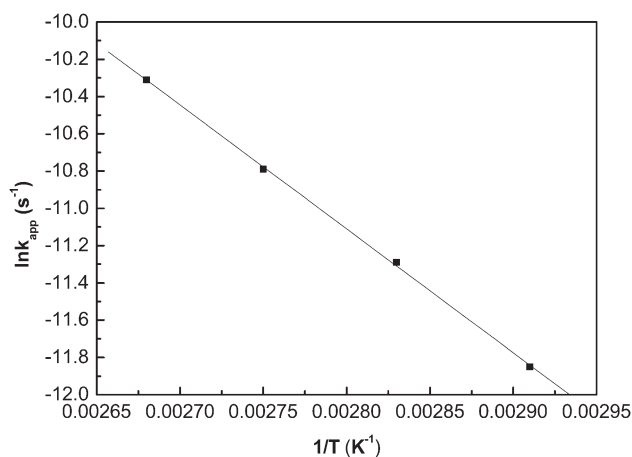


Figure 5. Effect of temperature on $\ln k_{app}$.

polymerization temperature on Fe-mediated ICAR ATRP of SAN in PEG-400 were investigated. The results are summarized in Table IV. From Table IV, it can be seen that the polymerization rate increased when the temperature was increased from 70 to 100°C. The conversion was achieved 48.62% within 26 h, 53.15% within 17 h, 52.33% within 10 h and 51.17% within 6 h, respectively. As evidenced by the apparent rate constant at different temperature (see Table IV). From Table IV, the apparent rate constant changed from $7.11 \times 10^{-6} \text{ s}^{-1}$ to $3.32 \times 10^{-5} \text{ s}^{-1}$ with increasing temperature from 70 to 100°C, which was due to the increase of both the radical propagation rate constant and the equilibrium constant. In the meantime, the M_w/M_n values of the obtained copolymer increased slightly from 1.20 to 1.34, indicating that the reaction temperature affected slightly the living characteristic of ICAR ATRP of St and AN. This may be that some terminations occurred at the higher temperature.

The activation energy is determined from the slope of the plot of the logarithm of the rate of reaction against the reciprocal of the absolute temperature. From Figure 5, the apparent activation energy was $55.67 \text{ kJ mol}^{-1}$.

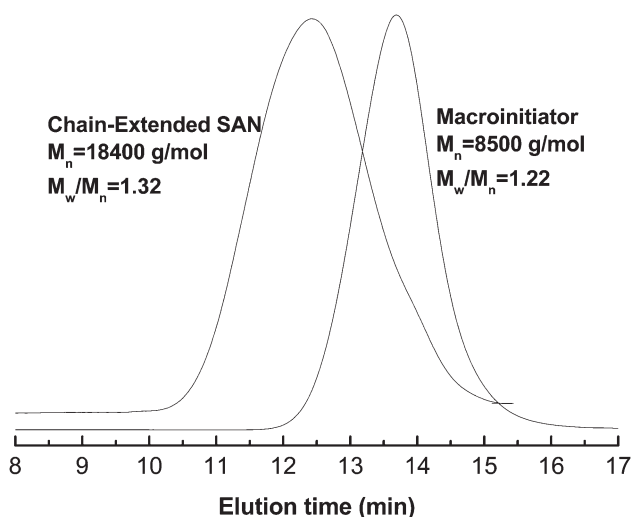


Figure 6. GPC curves of SAN before and after a chain extension reaction.

Chain Extension of SAN

To further investigate the “living” characteristics during the polymerization, chain extension experiment was performed with the resulting chlorine-terminated St as macroinitiator at 90°C in PEG-400 under stirring with the molar ratio of $[\text{St}]_0/[\text{AN}]_0/[\text{St-Cl}]_0/[\text{FeCl}_3 \cdot 6\text{H}_2\text{O}]_0/[\text{SA}]_0/[\text{AIBN}]_0 = 225 : 135 : 1 : 0.4 : 0.8 : 0.1$. Figure 6 depicts both GPC traces of the macroinitiator and the extended SAN copolymer. As shown in Figure 6, the M_n values changed from 8500 to 18,400 g mol^{-1} and M_w/M_n values changed from 1.22 to 1.32. Furthermore, the GPC curves were monomodal and symmetric, which clearly confirmed the occurrence of chain extension.

CONCLUSION

Fe-mediated ICAR ATRPs of SAN were successfully performed at 90°C in PEG-400 with CCl_4 as an initiator and $\text{FeCl}_3 \cdot 6\text{H}_2\text{O}/\text{SA}$ as a catalyst, AIBN as a thermal free radical initiator. Well-defined copolymers were obtained under these experimental conditions. The polymerization rate increased with temperature and the apparent activation energy was found to be $55.67 \text{ kJ mol}^{-1}$. The polymerization obeyed the first-order kinetics and molecular weight increased with conversion with narrow molecular weight distribution, indicating that the copolymerization of SAN was a controlled/“living” procedure. The chain extension further confirmed the “living”/controlled nature of the polymerization process.

ACKNOWLEDGMENTS

The authors are grateful for the financial support by Scientific Research Fund of Hunan Provincial Education Department (13A031, 12A134, and 13C364), the Science and Technology Planning Project of Hunan Province, China (Nos. 2012FJ4272), and the Open Foundation of Fine Petrochemical Catalytic and Separating Key Laboratory of Hunan Province.

REFERENCES

- Kato, M.; Kamigaito, M.; Sawamoto, M.; Higashimura, T. *Macromolecules* **1995**, *28*, 1721.
- Wang, J. S.; Matyjaszewski, K. *J. Am. Chem. Soc.* **1995**, *117*, 5614.
- Wang, J. S.; Matyjaszewski, K. *Macromolecules* **1995**, *28*, 7901.
- Percec, V.; Barboiu, B. *Macromolecules* **1995**, *28*, 7970.
- Mueller, L.; Jakubowski, W.; Tang, W.; Matyjaszewski, K. *Macromolecules* **2007**, *40*, 6464.
- Konkolewicz, D.; Magenau, A. J. D.; Averick, S. E.; Simakova, A.; He, H. K.; Matyjaszewski, K. *Macromolecules* **2012**, *45*, 4461.
- D'hooge, D. R.; Konkolewicz, D.; Reyniers, M.-F.; Marin, G. B.; Matyjaszewski, K. *Macromol. Theory Simul.* **2012**, *21*, 52.
- Dong, H. C.; Tang, W.; Matyjaszewski, K. *Macromolecules* **2007**, *40*, 2974.
- Tsarevsky, N. V.; Matyjaszewski, K. *Chem. Rev.* **2007**, *107*, 2270.

10. Zhu, G. H.; Zhang, L. F.; Zhang, Z. B.; Zhu, J.; Tu, Y. F.; Cheng, Z. P.; Zhu, X. L. *Macromolecules* **2011**, *44*, 3233.
11. Zhang, L.; Miao, J.; Cheng, Z.; Zhu, X. L. *Macromol. Rapid Commun.* **2010**, *31*, 275.
12. Wang, Y.; Zhang, Y.; Parker, B.; Matyjaszewski, K. *Macromolecules* **2011**, *44*, 4022.
13. Mukumoto, K.; Li, Y. C.; Nese, A.; Sheiko, S. S.; Matyjaszewski, K. *Macromolecules* **2012**, *45*, 9243.
14. Mukumoto, K.; Wang, Y.; Matyjaszewski, K. *ACS Macro Lett.* **2012**, *1*, 599.
15. Wang, G. X.; Lu, M.; Liu, Y. B. *J. Appl. Polym. Sci.* **2012**, *126*, 381.
16. Wang, G. X.; Lu, M.; Zhong, M.; Wu, H. *J. Polym. Res.* **2012**, *19*, 9782.
17. Wang, G. X.; Lu, M.; Hou, Z.-H.; Wu, H. *J. Polym. Res.* **2013**, *20*, 1.
18. Chandrasekhar, S.; Narsihmulu, C.; Shameem Sultana, S.; Ramakrishna Reddy, N. *ChemInform* **2003**, *34*, 4399.
19. Zhou, T.; Xiao, X. H.; Li, G. K.; Cai, Z. W. *J. Chromatogr. A* **2011**, *1218*, 3608.
20. Totten, G. E.; Clinton, N. A. *J. Macromol. Sci. Rev. Macromol. Chem. Phys.* **1988**, *C28*, 293.
21. Hsiao, H. C.; Weng, H. S. *J. Chem. Technol. Biotechnol.* **2001**, *76*, 959.
22. Hu, Z. Q.; Shen, X. R.; Qiu, H. Y.; Lai, G. Q. *Eur. Polym. J.* **2009**, *45*, 2313.
23. Perrier, S.; Gemici, H.; Li, S. *Chem. Commun.* **2004**, *4*, 604.
24. Garcia-Rubio, L. H.; Lord, M. G.; MacGregor, J. F.; Hamielec, A. F. *Polymer* **1985**, *26*, 2001.
25. Singh, A.; Kamal, M.; Singh, D. K. *J. Appl. Polym. Sci.* **2011**, *121*, 1052.
26. Lu, Q.; Weng, Z. X.; Shan, G. R.; Lai, G. Q.; Pan, Z. R. *J. Appl. Polym. Sci.* **2006**, *101*, 4270.
27. Nomura, M.; Liu, X.; Mizutani, F.; Sato, S.; Fujita, K. *Macromol. Symp.* **1995**, *92*, 232.
28. Lee, K. C.; Gan, L. M.; Chew, C. H.; Ng, S. C. *Polymer* **1995**, *36*, 3719.
29. Pietrasik, J.; Dong, H.C.; Matyjaszewski, K. *Macromolecules* **2006**, *39*, 6384.
30. Wang, G. X.; Lu, M.; Hou, Z. H.; Wu, H. *J. Polym. Res.* **2013**, *20*, 1.
31. Ilhanli, O. B.; Erdogan, T.; Tunca, U.; Hizal, G. *J. Polym. Sci. Part A: Polym. Chem.* **2006**, *44*, 3374.
32. Wang, G. X.; Lu, M. *e-Polymer* **2012**, 054.
33. Fan, D. Q.; He, J. P.; Xu, J. T.; Tang, W.; Liu, Y.; Yang, Y. L. *J. Polym. Sci. Part A: Polym. Chem.* **2006**, *44*, 2260.
34. Al-Harathi, M.; Sardashti, A.; Soares, J. B. P.; Simon, L. C. *Polymer* **2007**, *48*, 1954.
35. Wang, G. X.; Wu, H. *Polym. Bull.* **2011**, *67*, 1809.
36. Chen, Q. F.; Zhang, Z. B.; Zhou, N. C.; Cheng, Z. P.; Tu, Y. F.; Zhu, X. L. *J. Polym. Sci. Part A: Polym. Chem.* **2011**, *49*, 1183.